Journal of Metals, Materials and Minerals, 34(1), 1846, 2024

Integration of jackfruit seed-derived carbon dots and electronic nose for a sensitive detection of formaldehyde vapor

Thitarat PRATHUMSUWAN[1], Sumana KLADSOMBOON[2], Alfred Antony CHRISTY[3], Insik IN[4,5], Xiao LIANG[6], Shufeng SONG[7], Yao WANG[8,9], Thitirat INPRASIT[10], Peerasak PAOPRASERT[1,*], and Natee SIRISIT[1,*]

[1] *Department of Chemistry, Faculty of Science and Technology, Thammasat University, Pathumthani, 12120 Thailand*
[2] *Department of Radiological Technology, Faculty of Medical Technology, Mahidol University, Nakhon Pathom, 73170 Thailand*
[3] *Department of Science, Faculty of Engineering and Science, University of Agder, Kristiansand, Norway*
[4] *Department of IT Convergence (Brain Korea PLUS 21), Korea National University of Transportation, Chungju 380-702, South Korea*
[5] *Department of Polymer Science and Engineering, Korea National University of Transportation, Chungju 380-702, South Korea*
[6] *College of Chemistry and Chemical Engineering, Hunan University, Changsha, Hunan 410082, P. R. China*
[7] *College of Aerospace Engineering, Chongqing University, Chongqing 400044, China*
[8] *Guangdong Provincial Key Laboratory of Optical Information Materials and Technology, Institute of Electronic Paper Displays, South China Academy of Advanced Optoelectronics, South China Normal University, Guangzhou, 510006, China*
[9] *National Center for International Research on Green Optoelectronics, South China Normal University, Guangzhou, 510006, China*
[10] *Department of Materials and Textile Technology, Faculty of Science and Technology, Thammasat University, Pathumthani, 12120 Thailand*

***Corresponding author e-mail**: peerasak@tu.ac.th, snatee@staff.tu.ac.th

Received date:
19 September 2023
Revised date
3 January 2024
Accepted date:
12 January 2024

Keywords:
Carbon dot;
Electronic nose;
Formaldehyde;
Jackfruit seed

Abstract

The preparation of carbon dots from jackfruit seeds through a pyrolysis method at 280°C and their use for the detection of formaldehyde were reported. The as-prepared carbon dots showed a high fluorescence efficiency with a quantum yield of 12.7% and excellent photostability and dispersibility in aqueous solution with a zeta potential of –62.5 mV. The integration of carbon dot thin film and a home-made optical electronic nose system possessed sensitivity towards formaldehyde vapor with a detection limit of 24.7%v/v across a linear range of 25%v/v to 100%v/v. Furthermore, the sensor showed the highest sensitivity towards formaldehyde against other volatile organic compounds through a strong interaction between the carbonyl groups and the carbon dots. Additionally, principal component analysis (PCA) was conducted to achieve quantitative measurements of formaldehyde content in different formaldehyde volume ratios with substantial variance. Due to the significance of methanol as a typical chemical precursor for the industrial manufacturing of formaldehyde, the quantitative analytical method is essential to determining formaldehyde or methanol concentration. The sensing ability of carbon dot film-integrated electronic nose towards formaldehyde in formaldehyde/methanol mixtures was measured to be 10.74%v/v in a linear range of 25%v/v to 100%v/v. The PCA showed orderly linear combinations of the data set, which can be potentially utilized to analyze formaldehyde and methanol content in industrial processes. The results indicate the significant potential of carbon dots and optical electronic nose system as an effective formaldehyde sensing platform. Potential applications include the quantification of formaldehyde from methanol conversion and determination of methanol contaminant in formaldehyde.

1. Introduction

Formaldehyde (CH_2O), also known as methanal, is the smallest aldehyde compound and an important precursor or building block for various chemicals and a wide range of products. Formaldehyde and formaldehyde-based chemicals have also been used as components, adhesives, preservatives, and antibacterial agents in various household products, such as detergents, softeners, glues, paints, and carpet cleaners. In addition, formaldehyde-based resin materials offer insulating properties for flooring, furniture, wooden products, medium-density fiberboard, particleboard, wood cabinetry, and plywood [1]. Manufacturing of products involving formaldehyde as a reactant is the cause of formaldehyde releasing into indoor air due to its high volatility [2]. Formaldehyde can be naturally generated in bacteria, plants, and humans as a part of cellular metabolism [3]. Formaldehyde release through biogenic reactions and biomass burning, such as bushfires and forest [4], has been reported as an environmental contribution of increasing formaldehyde concentration.

The International Agency for Research on Cancer (IARC) under the WHO classified formaldehyde as a human carcinogen (Group 1). Several reviews reported that an formaldehyde exposure level between 0.15 mg·m^{-3} to 1.25 mg·m^{-3} can cause sensorial irritation [5-7]. The lowest concentration of formaldehyde to cause eye irritation is 0.38 mg·m^{-3} after 4 h exposure, thereby, increasing eyeblink frequencies and conjunctival redness appearance. Moreover, formaldehyde intake over 1.25 mg·m^{-3} can lead to the risk of nasopharyngeal cancer and possibly death at an exposure over 5 mg·m^{-3}. Due to the hazard of formaldehyde, analytical techniques are urgently needed to measure the amount of formaldehyde released for the assessment of human health effects.

In general, there are several analytical methods that can be used to measure formaldehyde quantities. For example, Fourier transform infrared spectroscopy (FT-IR), tunable diode laser spectroscopy (TDLS), and matrix isolation infrared have been reported as formaldehyde analytical techniques that showed the detection limit in the range of 0.03 ppb to 6.0 ppb [8]. Photoacoustic spectroscopy (PAS) can also be employed to measure indoor formaldehyde levels, reflecting good detection limits despite the presence of other pollutants in the air [9]. Derivatization is another analytical method that has been associated with chromatographic or spectroscopic techniques for analyzing the quantity of emitted formaldehyde. These techniques are highly suited to the determination of formaldehyde for indoor applications or formaldehyde batch samplings. However, the non-specificity of these techniques without applied chromatographic separation, inadequate sensitivity due to reactivity between most reagents and carbonyl compounds, and required toxic reagents are problems that have been commonly found in derivatization methods [10-12]. Sensors have become fascinating tools, providing simple and fast techniques for formaldehyde detection and evaluation. For example, gold-doped metal oxide mixtures [13] and palladium-doped tin oxide on a silicon substrate [14] have been utilized as micro-formaldehyde gas sensors, which are capable of detecting formaldehyde vapor with rapid response and recovery time. In addition, tin oxide doped with hydroxyl functionalized multi-walled carbon nanotubes was used as a semi-conductor gas sensor to determine gaseous indoor formaldehyde with a detection limit as low as 0.03 ppm [15]. Currently, nanotechnology has been of interest for fabricating formaldehyde sensors. The utilization of toxic reagents or heavy metals should be avoided due to human health and environmental concerns. Also, the cost effectiveness and simplicity of materials and instruments for formaldehyde detection should be concurrently considered. Therefore, in this work, nanosized carbon dots were chosen as sensing materials integrated with an electronic nose apparatus for formaldehyde detection.

Carbon dots (CDs) are carbonaceous nanomaterials with useful properties, including tunable fluorescence, photostability, and high biocompatibility, making them suitable for being employed as chemical- or biological- specified sensors. They can be easily synthesized via several approaches, such as pyrolysis, hydrothermal treatment, and microwave irradiation, using natural or waste precursors, for example, cranberry beans [16], lemon juice [17], and food waste [18]. These nanomaterials provide interesting and multifunctional applications, such as chemical [19] and biological sensing [20], drug delivery [21], photocatalysis [22], and electrocatalysis [23]. In this work, jackfruit seeds were used as precursors to synthesize carbon dots due to their high organic carbon contents. Moreover, the synthesis of carbon dots is an attractive and alternative way to reduce the jackfruit waste that increases from jackfruit consumption, especially in tropical countries [24].

The jackfruit seed-derived carbon dots were employed as a formaldehyde sensing material using an optical electronic nose (e-nose) as a gas sensing apparatus. The electronic nose system is a rapid and useful system that mimics human olfactory senses to sense a variety of vapors, depending on the applied sensing materials [25]. In this work, the electronic nose system was developed to monitor the change in optical transmission upon exposure to formaldehyde vapor in different concentrations and mixtures, using carbon dot film as sensing material. Principal component analysis (PCA) was employed to differentiate formaldehyde vapor from other targeted volatile organic compounds (VOCs). The correlation between sensor responses and concentrations of formaldehyde, which is combined with the PCA score plot, provides a quantitative method for formaldehyde analysis in aqueous and mixture solutions.

2. Experimental

2.1 Chemicals and materials

Jackfruit seeds were obtained from a local fruit market in Pathumthani, Thailand. They were thoroughly washed with water and ethanol several times and seed peels were removed. Jackfruit seeds were then cut into small pieces using a blender. The pieces of jackfruit seeds were subsequently dried overnight in the oven at 60°C for 24 h. Dried jackfruit seeds were ground to a fine powder prior to use. Chemicals, including potassium hydroxide, sulfuric acid, quinine sulfate dihydrate, formaldehyde, and acetaldehyde, were purchased from Sigma Aldrich and used as received without further purification. Nitric acid (65% HNO_3) and organic solvents were obtained from Carlo Erba. Cellulose dialysis membrane (1000 Da MWCO) was bought from Membrane Filtration Product, Inc. Deionized (DI) water with a resistance greater than 18 MΩ·cm^{-1} was used in all experiments.

2.2 Synthesis of carbon dots

The jackfruit seed powder (10.00 g) was suspended in DI water (60 mL) and mixed with 0.5 M nitric acid (60 mL). The mixture solution was then stirred at 900 rpm for 30 min to obtain a homogeneous solution. After stirring, the mixture solution was refluxed at 100°C for 24 h and then pyrolyzed at 280°C for 6 h. The remaining black solid products were dissolved in DI water (60 mL) and the solution was filtered to obtain the brown liquid. The brown liquid was subsequently dialyzed in a dialysis bag (1000 Da MWCO) for 72 h. The resulting solution was centrifuged at 10,000 rpm for 20 min to remove agglomerated particles. Finally, carbon dots in solid powder form (0.104 g, 1.04%) were obtained by freeze drying for 24 h.

2.3 Formaldehyde vapor detection and electronic nose setup

Carbon dot film was prepared on a glass slide (4 cm^2 × 4 cm^2) by casting a film of carbon dot solution (2.0 g·L^{-1}) and drying overnight at 80°C. The optical electronic nose system consists of light sources, carbon dot film as sensing material, and a photodetector. Light-emitting

diodes (LEDs) and a commercial photodetector (ET-TCS230) were used to detect light intensity. Eight gas sensor arrays were generated based on eight colors of LEDs, including infrared, red (638 nm), yellow (587 nm), green (537 nm), blue (457 nm), blue-green (472 nm), violet (399 nm), and white. The transmitted light intensity through a sensing film was observed in the form of photon frequency (Hz), captured by a photodetector [26]. All of the measurements were carried out at room temperature. The gas sensing capability of carbon dot films was examined under dynamic gas flow through a home-made chamber. Nitrogen gas (99.9%) was used as the reference and carrier with a flow rate of about 500 mL·min^{-1}. The sensor system was designed to switch between sample and reference gases for several cycles by a solenoid valve which was controlled by a computer program and data acquisition (DAQ) card. The DAQ card was connected to a photodetector to visualize the obtained absorption spectra on a computer. All obtained data is calculated using software based on the principal component analysis (PCA) procedure to convert a set of observations of correlated variables into a set of values of linearly uncorrelated variables, resulting in a PCA score plot.

A selectivity experiment was conducted using several solvent samples as vapor sources, including acetic acid, acetone, acetaldehyde, dichloromethane, DI water, ethanol, formaldehyde, methanol, and tetrahydrofuran. N_2 gas was alternately flowed as a reference for 120 s and as a carrier gas to carry solvent vapor for 60 s in each cycle, manipulating by the solenoid valves. The change in light transmission through carbon dot film was then recorded as a plot of signal response as a function of time. After six cycles of flowing reference gas and vapor samples, the sensor response was calculated as follows:

$$\text{Sensor response (\%)} = \left|\frac{I_{vapor} - I_R}{I_R}\right| \times 100$$

where I_{vapor} is the signal response of vapor samples and I_R is the signal response of N_2 gas.

The sensitivity of carbon dot film towards formaldehyde vapor generated from different concentrations of formaldehyde solutions (0, 25, 50, 75, and 100%v/v) was evaluated. The sensitivity of carbon dot film to formaldehyde was calculated by the following Equation:

$$\text{Sensitivity} = \left|\frac{I_{vapor} - I_R}{I_R}\right|$$

where I_{vapor} is the signal response of formaldehyde vapor and I_R is the signal response of N_2 gas.

Formaldehyde content in formaldehyde/methanol mixtures was further evaluated because of the significance of methanol as a commercial precursor for formaldehyde production. Formaldehyde (30%) and methanol were mixed at different volume ratios (0, 1, 5, 10, 25, 50, 75, and 100%v/v) to investigate the sensor responses of the carbon dot film toward the mixtures of formaldehyde/methanol.

2.4 Quantum yield measurements

The quantum yield ($\emptyset_X$) of the carbon dots was measured based on the slope method using quinine sulfate dihydrate as a fluorescence standard, following previous reports [27]. The equation for calculating the quantum yield is the following.

$$\emptyset_X = \emptyset_{ST}\left(\frac{Grad_X}{Grad_{ST}}\right)\left(\frac{\eta_X^2}{\eta_{ST}^2}\right)$$

where Grad is the gradient (slope) from the plot of the integrated fluorescence intensity and absorbance, and η is the refractive index of the solution. The subscripts ST and X denote the quinine sulfate and carbon dot aqueous solutions, respectively. Quinine sulfate in 0.1 M H_2SO_4 was used as a standard (ϕ_{ST} = 54% at 360 nm).

2.5 Characterization

Fourier transform infrared (FTIR) spectra were obtained using a Perkin Elmer FTIR spectrometer (Spectrum 2000) and KBr pellets. The surface elements were investigated using an X-ray photoelectron spectrometer (XPS) (AXIS ULTRA^{DLD}, Kratos Analytical Ltd., Manchester UK) with an X-ray spot size of 700 μm^2 × 300 μm^2 and monochromatic Al $K_{\alpha 1,2}$ (150 W). A carbon dot solution (0.1 g·L^{-1}) was prepared, dropped on a clean 1 cm^2 × 1 cm^2 glass slide, and then dried in an oven overnight at 60°C. Transmission electron microscopy (TEM) images were obtained using a JEOL JEM-2100 microscope. The average size of carbon dots was determined using ImageJ software. Samples were prepared by deposition of a carbon dot solution (1.0 g·L^{-1}) onto a copper grid coated with an ultra-thin film of carbon and dried by evaporation at 60°C. The ultraviolet-visible and fluorescence spectra were measured using a UV-visible spectrophotometer (Shimadzu, UV-1700 PharmaSpec) and a fluorescence spectrophotometer (Jasco, FP-6200), respectively. The zeta potential was measured using a dynamic light scatter (DLS) instrument (HORIBA, Nano Partica SZ-100) at 25°C. A carbon dot solution was prepared by dissolving carbon dots in DI water (1 g·L^{-1}) and ultrasonicated for 30 min. The viscosity, pH, and conductivity of carbon dot solution were 0.89 mPa·s^{-1}, 7, and 0.083 mS·cm^{-1}, respectively. The near-infrared spectrum of carbon dots was recorded using a Perkin Elmer Spectrum One NTS FT-NIR spectrometer equipped with a Perkin Elmer transflectance accessory and deuterated triglycine sulfate detector.

3. Results and discussion

3.1 Synthesis and characterization of carbon dots

The source of carbon and heteroatom dopants in starting materials is an important factor in producing the high fluorescence quantum yield of carbon dots [28]. Jackfruit seeds, which consist of carbohydrates, proteins, fats, and fibers, were chosen as the starting materials in this work. The synthetic route of the carbon dots is illustrated in Figure 1. Acid treatment was first applied to digest carbohydrates, proteins, fats, and fibers in jackfruit seeds into smaller molecules and to remove mineral impurities. The dark-brown solution was then pyrolyzed at 280°C for 6 h to obtain the black carbonized powder. After multiple steps of purification, the carbon dots were obtained as solid products with a fluorescence quantum yield of 12.7%, which is high compared to other natural seed-derived carbon dots (Table 1). This is due to the high nitrogen content in the jackfruit seeds, which is known to enhance the fluorescence quantum yield.

Table 1. Fluorescence quantum yields (QYs) of natural seed-derived carbon dots from previous studies and this work.

Precursor seed	Method	QY (%)	N content (%)	Ref.
Chia	Pyrolysis	24	0	[29]
Apple	Pyrolysis	20	5.4	[30]
Lychee	Pyrolysis	10.6	-	[31]
Fennel	Pyrolysis	9.5	0	[32]
Avocado	Carbonization	9.2	-	[33]
Sesame	Microwave-assisted pyrolysis	8.02	-	[34]
Fenugreek	Pyrolysis	7.5	-	[35]
Sunflower	Hydrothermal	3.58	17.88	[36]
Black sesame	Hydrothermal	2	9.0	[37]
Jackfruit	Acid treatment-assisted pyrolysis	12.7	5.64	This work

The particle size and morphology of the carbon dots synthesized in this work were determined using TEM. The TEM analysis of the carbon dots presented spherical-shaped particles with an average size of 2.97 nm and showed good dispersion, suggesting non-agglomerated carbon particles at the nanoscale (Figure 2(a) and Figure 2(b)). A lattice spacing of 0.34 nm was obtained from the high-resolution TEM image (inset), which is close to a lattice spacing of graphite. The zeta potential was –62.5 mV, indicating a negative charge on the surface functional groups of carbon dots and supporting the well dispersed carbon dot particles in aqueous solution. The highly negative charge on the surface arose from the existence of abundant negatively charged hydroxyl and carboxyl groups on the surface of carbon dots.

The FTIR spectrum of jackfruit seed-derived carbon dots was obtained to investigate the surface functional groups. As shown in Figure 2(c), the broad and strong signal at 3427 cm^{-1} was attributed to the stretching vibrations of O-H and N-H bonds of hydroxyl, carboxyl, and amino-containing functional groups [38]. The signal at 1611 cm^{-1} showed the vibration of C=C and C=O bonds, indicating the presence of the alkenyl and carbonyl functional groups [39]. The obvious signal at 1386 cm^{-1} corresponded to the bending vibration of the C-H bond, proving the existence of sp^3 hybridization in the alkyl functional groups [40].

The XPS technique was applied to investigate elemental compositions and chemical bonds within the carbon dots. From the XPS survey spectrum (Figure 3(a)), a ratio of carbon and oxygen contents in the carbon dots was higher than that of nitrogen content. The carbon dots produced signals at 286.0 eV, 400.0 eV, and 533.0 eV. These peaks were attributed to C_{1s}, N_{1s}, and O_{1s}, with atomic concentrations of 61.98%, 5.64%, and 28.53%, respectively (Figure 3(a)). The high-resolution C_{1s} (Figure 3(b)) and O_{1s} spectra (Figure 3(c)) presented a higher intensity of hydroxyl and carbonyl functional groups than amine functional groups in the N_{1s} spectra (Figure 3(d)) which represent negatively charged species in the carbon dot solution [41]. The high-resolution spectrum of C_{1s} peak (Figure 3(b)) was deconvoluted into four peaks at 284.8, 286.0, 287.5, and 288.9 eV, corresponding to the C-C, C-N, C=N/C=O, and O=C-OH functional groups, respectively [33,42-44]. As shown in Figure 3(c), the peaks centered at 531.2 eV, 532.2 eV, 533.3 eV, and 534.3 eV of the O_{1s} spectrum can be assigned to C=O, C-O, C-OH/C-O-C, and O=C-OH bonds, respectively [45-47]. The high-resolution spectrum of N_{1s} was fitted into three peaks at 399.0 eV, 400.2 eV, and 401.4 eV, corresponding to the pyridinic-N, graphitic-N, and pyrrolic-N, respectively (Figure 3(d)). These results revealed the existence of oxygen- and nitrogen-containing functional groups in carbon dots, correlating with the FTIR results

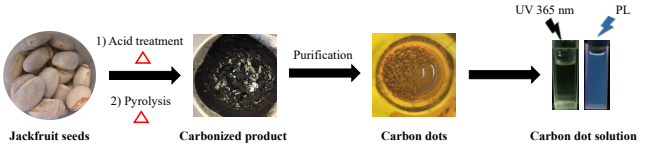

Figure 1. Schematic illustration for the preparation of the carbon dots from jackfruit seeds.

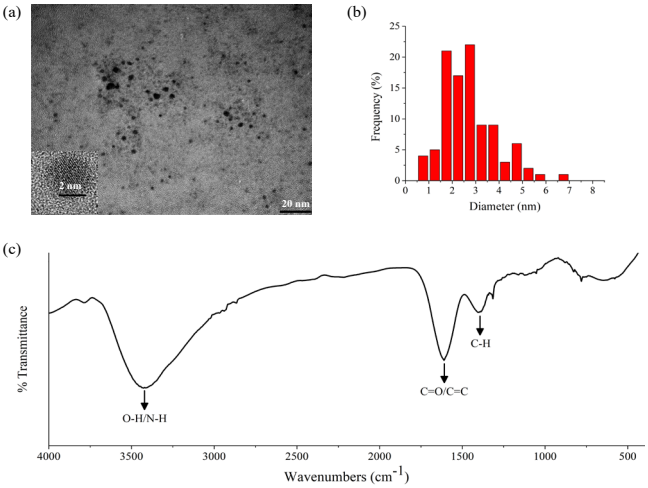

Figure 2. (a) TEM image of the carbon dots derived from jackfruit seeds, (b) their size distribution diagram, and (c) FTIR spectrum of the jackfruit seed-derived carbon dots.

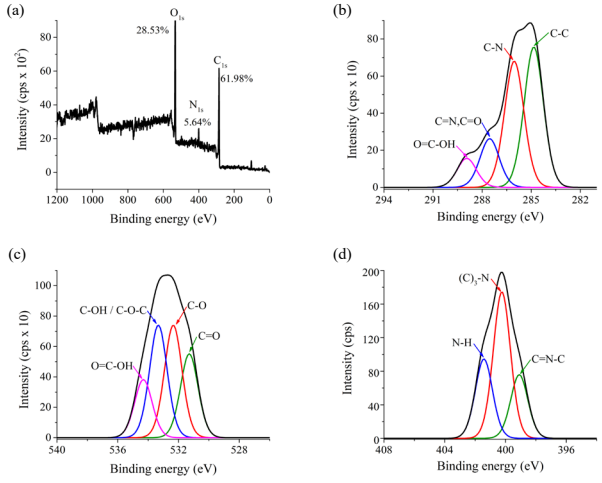

Figure 3. (a) Survey XPS spectrum of the carbon dots and high-resolution spectra corresponding to (b) C_{1s}, (c) O_{1s}, and (d) N_{1s} regions.

3.2 Optical properties

The optical properties of carbon dots were investigated through the observation of absorption and fluorescence emission spectra. The inset in Figure 4(a) shows photographs of the carbon dot solution under visible light and UV light (365 nm), indicating excellent dispersibility of carbon dot particles and showing blue fluorescence emission under UV exposure. The absorption spectrum (black line, Figure 4(a)) revealed a strong absorption between 200 nm to 250 nm, corresponding to the π-π^* electronic transition of the sp^2 aromatic system within the carbon core [48]. An intense fluorescence intensity was observed at 483 nm when the carbon dot solution was excited at 360 nm, verifying a superior blue emission color. This result is consistent with the average particle size of the obtained carbon dots, which was approximately 2 nm to 3 nm and typically related to blue fluorescence emission [49]. Furthermore, the excitation-dependent emission was demonstrated in Figure 4(b). The fluorescence emission peak was red shifted when the excitation wavelength was increased. This photoluminescence behavior is often found in carbon dots, which present several functional groups on their surface, creating multiple photoluminescence centers and energy levels. A multi-color fluorescence emission of carbon dots has been consequently controlled by varying excitation wavelengths without modifying their chemical structures, providing advantages in a wide range of bioimaging applications.

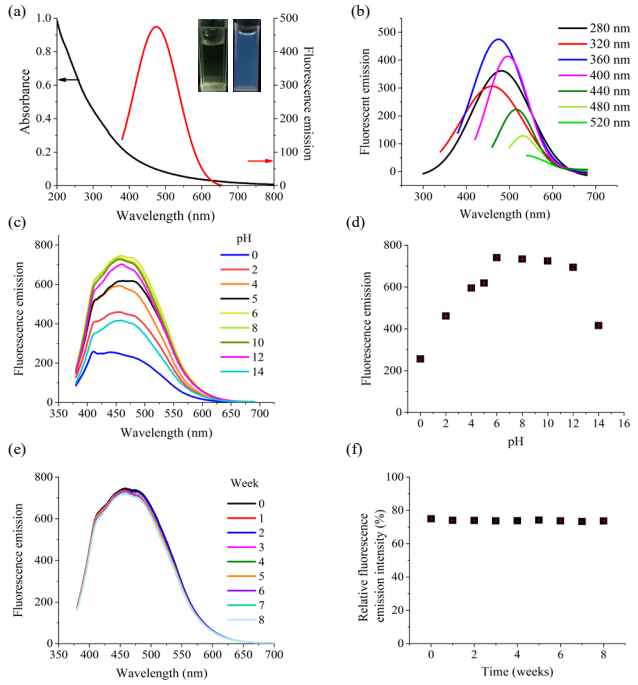

Figure 4. (a) Absorbance (black line) and fluorescence emission spectra of the carbon dots in aqueous solution (1.0 g·L^{-1}) (red line, λ_{ex} = 360 nm, λ_{em} = 380 nm to 700 nm). Insets present photographs of carbon dot solution under visible light (left) and UV light (right) and (b) excitation-dependent emission spectra of carbon dots (λ_{ex} = 280, 320, 360, 400, 480, and 520 nm). (c) Fluorescence spectra and (d) plots of fluorescence intensity of the carbon dots in aqueous solution (1.5 g·L^{-1}) at different pH levels, (e) and (f) fluorescence emission spectra and plots of relative fluorescence intensity (%) as a function of time (week). (λ_{ex} = 360 nm, λ_{em} = 380 nm to 700 nm, error bars showed standard deviations based on three independent measurements.)

The pH-dependent photoluminescence of the carbon dots was investigated (Figure 4(c) and Figure 4(d)). The fluorescence emission intensity dropped to 65% and almost 50% when the carbon dots were dispersed in severe acidic and basic solutions, respectively. This is due to the protonation of carboxyl groups in the acidic environment, which resulted in the agglomeration of carbon dots in the aqueous solution and the lower fluorescence efficiency. The decrease in fluorescence emission in strong basic solution (pH 14) might be due to the reduction in emissive sites on the particles [50]. In strong basic solutions, functional groups, such as carboxyl and hydroxyl groups, were deprotonated, which became less photoluminescent than in neutral state. The deprotonated carboxyl and hydroxyl groups led to a change in emissive states, resulting in a lower fluorescence intensity. Therefore, a suitable pH range is between 6 and 12. The different pH conditions of carbon dot solutions affected their fluorescence properties because of the existence of different surface charges on carbon dot particles, leading to the distribution of surface state energy levels [51]. In addition, the photostability of the as-prepared carbon dots was next examined by comparing it to the fluorescence emission of a standard fluorophore (quinine sulfate dihydrate) following this equation. Quinine sulfate was chosen as a benchmark because it is a stable compound.

$$\text{Relative fluorescence intensity emission} = \left(\frac{\text{Fluorescence intensity emission of carbon dots}}{\text{Fluorescence intensity emission of quinine sulfate}}\right) \times 100$$

The fluorescence intensity of carbon dots showed excellent photostability for at least eight weeks under ambient conditions (Figure 4(e) and Figure 4(f)). The relative fluorescence emission intensity of the carbon dots was about 75% with respect to that of quinine sulfate and remained at about that value throughout the 8 week period. With a long shelf life, the carbon dots prepared in this work can thus be kept for use for a long period of time.

3.3 Formaldehyde vapor detection

Since carbon dots have emerged as interesting fluorescence nanomaterials, their unique optical properties and hydrophilicity have been employed to detect several kinds of chemicals via interactions between conjugated π electronic systems/surface functional groups and electron donors or acceptors of analytes [52]. To evaluate the sensing capability of carbon dots towards volatile organic compounds (VOCs), optical electronic nose (e-nose) has been utilized to reliably mimic a biological nose. The sensory system of e-nose uses a transducer and data processing unit to detect odorant molecules and convert the data into sensing signal. In the sensory system, sensing elements with a wide range of absorption for a specific gas are essential and required. In this work, carbon dots were used as thin film sensors to detect formaldehyde vapor, which was generated from formaldehyde solutions and mixtures. The carbon dot film was prepared on a glass slide, which appeared a dark brown color, and placed inside a chamber with gas inlet and outlet (Figure 5). The carbon dot film was stable throughout the measurements and offered adequate absorption in the UV and visible regions. The electronic nose system, which consists of a flow system, LED light sources, photodetector, and a data processing unit, was used to measure

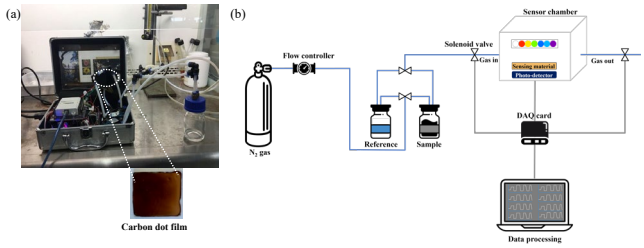

Figure 5. Photo of optical e-nose (a) and (b) setup diagram.

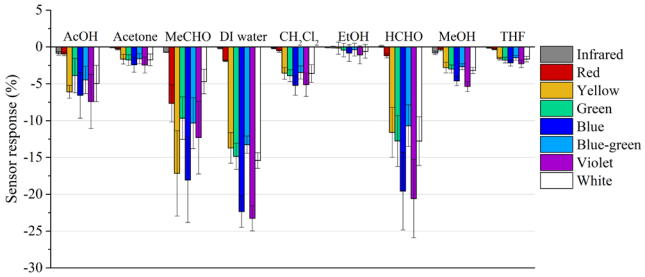

Figure 6. Comparison of sensor responses of the carbon dot film towards different solvent vapors using eight light sources.

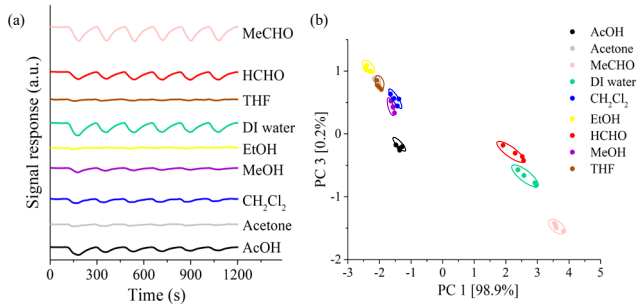

Figure 7. (a) Gas sensing response under red light (638 nm) and (b) PCA two-dimensional score plots of the carbon dot film upon exposure to different solvents, including acetaldehyde (MeCHO), formaldehyde (HCHO), tetrahydrofuran (THF), DI water, ethanol (EtOH), methanol (MeOH), dichloromethane (CH_2Cl_2), acetone, and acetic acid (AcOH), a flow rate of 60 mL·min^{-1}.

the light absorption and convert it into a signal response. Signal response is a change in absorption of carbon dot thin film after flowing formaldehyde vapor and N_2 as sample and reference gases, respectively. All data obtained in the sensing experiments was analyzed using software based on principal component analysis (PCA). PCA is a method that is utilized to minimize feature redundancy and filter out noise.

First, the as-prepared carbon dot thin film was used to detect various kinds of vapors by utilizing the solvents as vapor sources, including acetic acid, acetone, acetaldehyde, dichloromethane, DI water, ethanol, formaldehyde, methanol, and tetrahydrofuran, which are commonly and widely used in laboratories and industries. The carbon dot thin film was placed in a home-made chamber that consisted of eight light sources and a photodetector. Being manipulated by solenoid valves, the nitrogen gas was then alternately flowed for 120 s and carrier gas to carry vapor samples for 60 s in each cycle. The change in light transmission through the carbon dot thin film was subsequently recorded as a plot of signal response as a function of time (Figure 6). The light transmission dropped significantly when acetaldehyde, formaldehyde, DI water, and acetic acid vapors were switched on and flowed into the chamber while other solvents produced smaller signal response decreases.

As shown in Figure 7a, six cycles of flowing reference gas and vapor samples were carried out to demonstrate the reproducibility of the signals. After six cycles of flowing reference gas and vapor samples, the sensor response in percentage was calculated. it was found that the sensor responses of acetaldehyde, formaldehyde, and DI water were the three highest in value (0.208, 0.216, and 0.246, respectively). To clearly distinguish sample vapors, principal component analysis (PCA) was applied to manage the input data from eight light sources. The resulting data showed a score plot, and a circle was used to mark the exclusive zone of each vapor sample. The PCA score plot (Figure 7(b)) was obtained, verifying the separation of formaldehyde, acetaldehyde, DI water, ethanol, and methanol with excellent total variability of 98.9%. This suggests that our carbon dots can differentiate formaldehyde, acetaldehyde, and DI water from the rest of the solvent samples. We believe that the sensitivity towards these analytes arose from the polar-polar interactions between the carbon dots and the analytes, in particular, the aldehyde compounds. The carbonyl groups of formaldehyde and acetaldehyde and carbon dots could be responsible for the interactions. Along with these interactions, these aldehydes are volatile, allowing them to easily be in vapor phase and transported to the carbon dot film. Regarding the sensitivity towards water, the hydrogen bonding could be responsible for the strong interactions with the carbon dots as they possessed various hydrophilic functional groups, including carboxyls and hydroxyls. Consequently, the aldehyde compounds and water generated strong signals, when compared to other solvents.

Since formaldehyde is widely used in industrial production and provided one of the highest signal responses among VOCs (Figure 7), we would like to further test the sensing capability of the carbon dots towards formaldehyde in aqueous solutions at different concentrations. Formaldehyde aqueous solutions (0, 25, 50, 75, and 100%v/v) were used as vapor sources. The 100%v/v of formaldehyde solution produced the greatest magnitude of the signal response, and the signal response decreased as a function of decreasing formaldehyde concentration (Figure 8(a)). However, the carbon dot thin film still showed a signal response even though pure water (0%v/v concentration) was used as a sample. This was due to the high sensitivity of the carbon dots towards DI water because of their hydrophilicity. This was further confirmed by the presence of two peaks in the near-infrared spectra of our carbon dots at 5168 cm^{-1} and 4360 cm^{-1}, corresponding to water and bonded water to the carbonyl groups, respectively (Figure 8(d)) [53,54]. Therefore, the carbon dots could absorb and interact with water molecules even in a solid powder form. When nitrogen gas was flowed after the exposure of formaldehyde (100%v/v), the light transmission recovered in 97.7 s ± 5.4 s. The alternate flow between nitrogen gas and formaldehyde vapor was repeated multiple times, and neither degeneration of physical appearance nor decay of signal response was observed. This suggested that our carbon dots presented excellent repeatability as formaldehyde vapor sensing materials. In addition, the signal responses from eight light sources were subjected to PCA to get new representation data as a score plot. The score plot, obtained by selecting the data from the first two principal components (PC1 and PC2), gave a high value of 97.9% of the variance in the original data set with no overlap of exclusive zones (Figure 8(b)). The results

can be described that our carbon dots incorporated with the electronic nose system were able to reliably identify different concentrations of formaldehyde. This will be an applicable technique to measure the content of formaldehyde in chemical or industrial production lines. The calculated sensor responses from the difference in light transmission between the flows of nitrogen and formaldehyde were used to generate the plot as a function of formaldehyde concentration in solutions (Figure 8(c)). A Stern-Volmer plot as an inset of Figure 8(c) showed a well-pronounced linear relationship (R^2=0.9956) between sensor response and amount of formaldehyde across the range 25%v/v to 100%v/v formaldehyde. Notably, the calculated sensor response is based on the data generated from the green light array (537 nm) because of its highest magnitude of signal response during the alternate flows of reference gas and formaldehyde vapor (Table S2). The detection limit was calculated based on 3σ/slope method to be 24.7%v/v. Our detection limit was equivalent to 60.39 mg·kg^{-1} of formaldehyde, which is sufficient detectability to measure contaminate formaldehyde found in different seafood species in previous reports such as squid [55], giant tiger prawn [56], and main traded fish [57]. Despite a relatively high detection limit, this confirmed that our carbon dots-integrated electronic nose is a useful sensor for formaldehyde detection and provided an alternative quantifying method to measure the content of formaldehyde in aqueous solution. Furthermore, our work is the first to report the use of optical electronic nose for the detection of formaldehyde (Table 2). Although the sensing performance of our sensor needs further improvement to compete with others, the straightforward preparation of carbon dots, the utilization of biowaste, and the low cost of electronic nose system, compared to other sensing platforms, present the potential of our system for real applications, such as the quantification of formaldehyde from methanol conversion and determination of methanol contaminant in formaldehyde.

In the chemical industry, formaldehyde is widely synthesized from methanol through catalytic oxidation and dehydrogenation. We therefore examined the sensitivity of our carbon dots towards formaldehyde vapor in formaldehyde/methanol mixtures at various ratios (0, 1, 5, 10, 25, 50, 75, and 100%v/v). The optical transmission of carbon dot film was dramatically reduced when the flow system was switched from nitrogen gas to vapors from the formaldehyde/methanol mixtures (Figure 9(a)). To differentiate the formaldehyde content in various volume ratios of mixture solutions, PCA was employed to reduce high dimensional data into a score plot. Figure 9(b) obviously showed the separation of each concentration of formaldehyde/methanol mixtures from 5%v/v to 100%v/v based on the first two principal components (PC1 and PC2) with a substantial variance of 99.5% and 0.3%, respectively. The PCA result suggested that our carbon dot film-integrated optical electronic nose can be utilized to analyze formaldehyde and methanol content during oxidative hydrogenation reactions in industrial processes in which the score plots of the formaldehyde/methanol mixture are separated from 5% formaldehyde to 100% formaldehyde. Hence, the carbon dots could distinguish different ratios between formaldehyde and methanol between 5% to 100%. The sensor response increased with the concentration of formaldehyde, indicating the carbon dots were more sensitive to formaldehyde than methanol, which is consistent with Figure 7 (Figure 9(c) and Figure 9(d)). Based on the linear range from 25% to 100%, the limit of detection was determined, calculated from 3σ/slope method to evaluate the detectability of the minimum amount of formaldehyde in the mixture, to be 10.74%v/v. Therefore, the integration of our carbon dots and electronic nose apparatus can achieve the detection of formaldehyde in a formaldehyde/methanol mixture, expanding the practical uses of formaldehyde and methanol manufacturing.

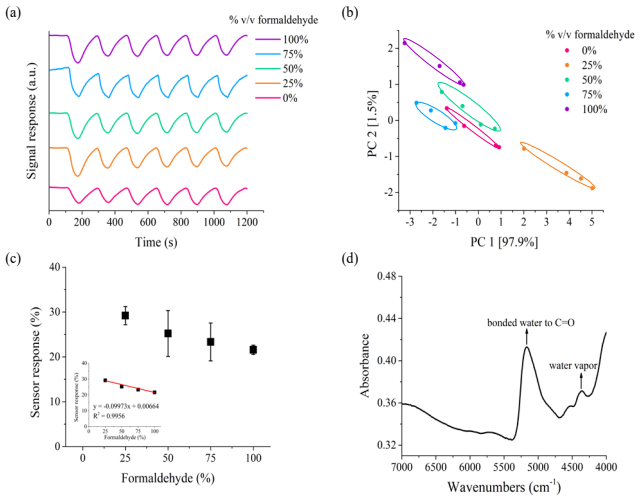

Figure 8. (a) Gas sensing response of the carbon dot film upon exposure to formaldehyde in different concentrations from a green light source (537 nm), (b) PCA two-dimensional score plots from various concentrations of formaldehyde, (c) Stern-Volmer plots of sensor response as a function of formaldehyde concentration with a linear range as inset (error bars represent standard deviations based on six cycles of vapor exposure), and (d) near-infrared spectrum of the jackfruit seed-derived carbon dots.

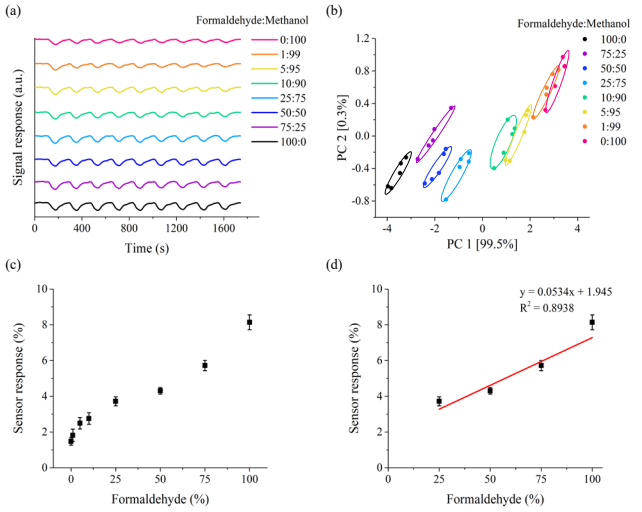

Figure 9. Gas sensing response (a) and (b) PCA two-dimensional plot of the carbon dot film upon exposure to a formaldehyde/methanol mixture in different volume ratio concentrations from a green light source (537 nm), (c) Stern-Volmer plots of sensor response as a function of formaldehyde concentration in formaldehyde/methanol solutions with a linear range as (d) (error bars represent standard deviations based on six cycles of vapor exposure).

Table 2. Summary of formaldehyde sensing systems.

Source of carbon dots	Synthesis methods	Formaldehyde detection method	LOD	Linear range	Ref
Jackfruit seeds	Pyrolysis	Optical electronic nose	24.7% v/v	25% v/v to 100%v/v	This work
L-ascorbic acid and ethylene glycol	Hydrothermal	Intelligent gas sensing platform (CGS-MT)	0.5 ppm	-	[58]
Citric acid monohydrate and ethylenediamine	Hydrothermal	Fluorescence spectrophotometer	22 $\mu g \cdot L^{-1}$	36.0 $\mu g \cdot L^{-1}$ to 270.0 $\mu g \cdot L^{-1}$	[59]
Lignin and *m*-phenylenediamine	Hydrothermal	Fluorescence spectrophotometer	7.40 $\mu g \cdot L^{-1}$	0.02 $mg \cdot L^{-1}$ to 1 $mg \cdot L^{-1}$	[60]
Laurel leaves	Hydrothermal	Quartz crystal microbalance sensor	0.34 $mg \cdot L^{-1}$	-	[61]
o-Phenylenediamine	Hydrothermal	Resonance light scattering technique	1.6 nM	4 nM to 1.6 mM	[62]
Purslane leaves	Hydrothermal	Quartz crystal microbalance sensor	42.61 Hz $mg^{-1} \cdot L^{-1}$	2.9 $mg \cdot L^{-1}$ to 23.2 $mg \cdot L^{-1}$	[63]
N-(phosphonomethyl) iminodiacetic acid and branched polyethyleneimine	Hydrothermal	Fluorescence spectrophotometer	0-40 µM	0.47 µM	[64]

4. Conclusions

In summary, carbon dots with high fluorescence efficiency, good dispersibility, and photostability were successfully synthesized by the acid treatment-assisted pyrolysis method using jackfruit seeds as available natural wastes as precursors. The incorporation of carbon dots and an optical electronic nose system renders a sensitive formaldehyde sensor as sensitive as 24.7%v/v, which is sufficient to use as a formaldehyde probe sensor in different seafood species. Moreover, the utilization of carbon dots as sensing materials presents the distinguishability of formaldehyde concentrations in aqueous and methanol-mixture solutions through PCA analysis. Our natural waste-derived carbon dots provide a foundation for a convenient and practical approach to the quality control of food and industrial products.

Acknowledgement

This research is financially supported by Thammasat University Research Unit in Carbon Materials and Green Chemistry Innovations and Thammasat University (contract No. TUGG102/2562). The authors gratefully express appreciation to the Department of Radiological Technology, Faculty of Medical Technology, and Mahidol University for the corporation and support in electronic nose experiments. T. Prathumsuwan is supported by Science Achievement Scholarships of Thailand.

References

[1] T. Salthammer, S. Mentese, and R. Marutzky, "Formaldehyde in the indoor environment," (in eng), *Chemical Reviews,* vol. 110, no. 4, pp. 2536-2572, 2010.

[2] X. Tang, Y. Bai, A. Duong, M. T. Smith, L. Li, and L. Zhang, "Formaldehyde in China: Production, consumption, exposure levels, and health effects," *Environment International,* vol. 35, no. 8, pp. 1210-1224, 2009.

[3] K. Tulpule, M. C. Hohnholt, and R. Dringen, "Formaldehyde metabolism and formaldehyde-induced stimulation of lactate production and glutathione export in cultured neurons," (in eng), *Journal of neurochemistry,* vol. 125, no. 2, pp. 260-72, 2013.

[4] Y. Zhang, R. Li, Q. Min, H. Bo, Y. Fu, Y. Wang, and Z. Gao, "The controlling factors of atmospheric formaldehyde (HCHO) in Amazon as seen from satellite," *Earth and Space Science,* vol. 6, no. 6, pp. 959-971, 2019.

[5] D. A. Kaden, C. Mandin, G. D. Nielsen, and P. Wolkoff, G. W. H. Organization, Ed. *WHO Guidelines for Indoor Air Quality: Selected Pollutants.* Scherfigsvej 8DK-2100 Copenhagen Ø, Denmark: WHO Regional Office for Europe, 2010, p. 454.

[6] J. H. E. Arts, M. A. J. Rennen, and C. de Heer, "Inhaled formaldehyde: Evaluation of sensory irritation in relation to carcinogenicity," *Regulatory Toxicology and Pharmacology,* vol. 44, no. 2, pp. 144-160, 2006.

[7] D. Paustenbach, Y. Alarie, T. Kulle, N. Schachter, R. Smith, J. Swenberg, and S. B. Horowitz, "A recommended occupational exposure limit for formaldehyde based on irritation," (in eng), *Journal of toxicology and environmental health,* vol. 50, no. 3, pp. 217-63, 1997.

[8] B. J. Finlayson-Pitts, and J. N. Pitts, "CHAPTER 3 - Spectroscopy and Photochemistry: Fundamentals," in *Chemistry of the Upper and Lower Atmosphere*, B. J. Finlayson-Pitts and J. N. Pitts Eds. San Diego: Academic Press, 2000, pp. 43-85.

[9] U. Krüger, M. Kraenzmer, and O. Strindehag, "Field studies of the indoor air quality by photoacoustic spectroscopy," *Environment International,* vol. 21, no. 6, pp. 791-801, 1995.

[10] T. Salthammer, S. Mentese, and R. Marutzky, "Formaldehyde in the Indoor Environment," *Chemical Reviews,* vol. 110, no. 4, pp. 2536-2572, 2010.

[11] J. B. de Andrade, and R. L. Tanner, "Determination of formaldehyde by HPLC as the DNPH derivative following high-volume air sampling onto bisulfite-coated cellulose filters," *Atmospheric Environment. Part A. General Topics,* vol. 26, no. 5, pp. 819-825, 1992.

[12] R. R. Miksch, D. W. Anthon, L. Z. Fanning, C. D. Hollowell, K. Revzan, and J. Glanville, "Modified pararosaniline method for the determination of formaldehyde in air," *Analytical Chemistry,* vol. 53, no. 13, pp. 2118-2123, 1981.

[13] J. Xu, X. Jia, X. Lou, G. Xi, J. Han, and Q. Gao, "Selective detection of HCHO gas using mixed oxides of ZnO/$ZnSnO_3$," *Sensors and Actuators B: Chemical,* vol. 120, no. 2, pp. 694-699, 2007.

[14] J. Wang, P. Zhang, J.-Q. Qi, and P.-J. Yao, "Silicon-based micro-gas sensors for detecting formaldehyde," *Sensors and Actuators B: Chemical,* vol. 136, no. 2, pp. 399-404, 2009.

[15] J. Wang, L. Liu, S.-Y. Cong, J.-Q. Qi, and B.-K. Xu, "An enrichment method to detect low concentration formaldehyde," *Sensors and Actuators B: Chemical,* vol. 134, no. 2, pp. 1010-1015, 2008.

[16] M. Zulfajri, G. Gedda, C.-J. Chang, Y.-P. Chang, and G. G. Huang, "cranberry beans derived carbon dots as a potential fluorescence sensor for selective detection of Fe^{3+} Ions in aqueous solution," *ACS Omega,* vol. 4, no. 13, pp. 15382-15392, 2019.

[17] A. Tadesse, M. Hagos, D. RamaDevi, K. Basavaiah, and N. Belachew, "Fluorescent-nitrogen-doped carbon quantum dots derived from citrus lemon juice: green synthesis, mercury(ii) ion sensing, and live cell imaging," *ACS Omega,* vol. 5, no. 8, pp. 3889-3898, 2020.

[18] Y. Zhou, Y. Liu, Y. Li, Z. He, Q. Xu, Y. Chen, J. Street, H. Guo, and M. Nelles, "Multicolor carbon nanodots from food waste and their heavy metal ion detection application," *RSC Advances,* 10.1039/C8RA03272F vol. 8, no. 42, pp. 23657-23662, 2018.

[19] T. K. Mondal, A. Kapuria, M. Miah, and S. K. Saha, "Solubility tuning of alkyl amine functionalized carbon quantum dots for selective detection of nitroexplosive," *Carbon,* vol. 209, p. 117972, 2023.

[20] Y.-F. He, K. Cheng, Z.-T. Zhong, X.-L. Hou, C.-Z. An, J. Zhang, W. Chen, B. Liu, J. Yuan, and Y-D. Zhao. "Carbon quantum dot fluorescent probe for labeling and imaging of stellate cell on liver frozen section below freezing point," *Analytica Chimica Acta,* vol. 1260, p. 341210, 2023.

[21] L. Wang, H. Pan, D. Gu, P. Li, Y. Su, and W. Pan, "A composite System combining self-targeted carbon dots and thermo-sensitive hydrogels for challenging ocular drug delivery," *Journal of Pharmaceutical Sciences,* vol. 111, no. 5, pp. 1391-1400, 2022.

[22] D. Xu, Y. Huang, Q. Ma, J. Qiao, X. Guo, and Y. Wu, "A 3D porous structured cellulose nanofibrils-based hydrogel with carbon dots-enhanced synergetic effects of adsorption and photocatalysis for effective Cr(VI) removal," *Chemical Engineering Journal,* vol. 456, p. 141104, 2023.

[23] T. Jorn-am, W. Pholauyphon, P. Supchocksoonthorn, N. Sirisit, C. Chanthad, J. Manyam, X. Liang, S. Song, and P. Paoprasert, "High-performance supercapacitors using synergistic hierarchical Ni-doped copper compounds/activated carbon composites with MXenes and carbon dots as simultaneous performance enhancers," *Electrochimica Acta,* vol. 447, p. 142147, 2023.

[24] J. L. F. Alves, J. C. G. da Silva, G. D. Mumbach, M. D. Domenico, V. F. da Silva Filho, R. F. de Sena, R. A. F. Machado, and C. Marangoni, "Insights into the bioenergy potential of jackfruit wastes considering their physicochemical properties, bioenergy indicators, combustion behaviors, and emission characteristics," *Renewable Energy,* vol. 155, pp. 1328-1338, 2020.

[25] X. Liu, S. Cheng, H. Liu, S. Hu, D. Zhang, and H. Ning, "A survey on gas sensing technology," (in eng), *Sensors (Basel, Switzerland),* vol. 12, no. 7, pp. 9635-65, 2012.

[26] S. Kladsomboon, M. Lutz, T. Pogfay, T. Puntheeranurak, and T. Kerdcharoen, "Hybrid optical-electrochemical electronic nose system based on Zn-porphyrin and multi-walled carbon nanotube composite," (in eng), *Journal of nanoscience and nanotechnology,* vol. 12, no. 7, pp. 5240-4, 2012.

[27] T. Prathumsuwan, S. Jamnongsong, S. Sampattavanich, and P. Paoprasert, "Preparation of carbon dots from succinic acid and glycerol as ferrous ion and hydrogen peroxide dual-mode sensors and for cell imaging," *Optical Materials,* vol. 86, pp. 517-529, 2018.

[28] N. K. Khairol Anuar, H. L. Tan, Y. P. Lim, M. S. So'aib, and N. F. Abu Bakar, "A review on multifunctional carbon-dots synthesized from biomass waste: Design/fabrication, characterization and applications," (in English), *Frontiers in Energy Research,* Review vol. 9, 2021.

[29] S. S. Jones, P. Sahatiya, and S. Badhulika, "One step, high yield synthesis of amphiphilic carbon quantum dots derived from chia seeds: a solvatochromic study," *New Journal of Chemistry,* 10.1039/C7NJ03513F vol. 41, no. 21, pp. 13130-13139, 2017.

[30] A. Chatzimarkou, T. G. Chatzimitakos, A. Kasouni, L. Sygellou, A. Avgeropoulos, and C. D. Stalikas, "Selective FRET-based sensing of 4-nitrophenol and cell imaging capitalizing on the fluorescent properties of carbon nanodots from apple seeds," *Sensors and Actuators B: Chemical,* vol. 258, pp. 1152-1160, 2018.

[31] M. Xue, M. Zou, J. Zhao, Z. Zhan, and S. Zhao, "Green preparation of fluorescent carbon dots from lychee seeds and their application for the selective detection of methylene blue and imaging in living cells," *Journal of Materials Chemistry B,* 10.1039/C5TB01073J vol. 3, no. 33, pp. 6783-6789, 2015.

[32] A. Dager, T. Uchida, T. Maekawa, and M. Tachibana, "Synthesis and characterization of Mono-disperse Carbon Quantum Dots from Fennel Seeds: Photoluminescence analysis using Machine Learning," *Scientific Reports,* vol. 9, no. 1, p. 14004, 2019.

[33] X. Wang, P. Yan, P. Kerns, S. Suib, L. M. Loew, and J. Zhao, "Voltage-dependent photoluminescence of carbon dots," *Journal of The Electrochemical Society,* vol. 167, no. 14, p. 147515, 2020.

[34] V. Roshni, and O. Divya, "One-step microwave-assisted green synthesis of luminescent n-doped carbon dots from sesame seeds for selective sensing of Fe(III)," *Current Science,* vol. 112, p. 385, 2017.

[35] N. Urushihara, T. Hirai, A. Dager, Y. Nakamura, Y. Nishi, K. Inoue, R. Suzuki, M. Tanimura, K. Shinozaki, and M. Tachibana, "Blue–green electroluminescent carbon dots derived from fenugreek seeds for display and lighting applications," *ACS Applied Nano Materials,* vol. 4, no. 11, pp. 12472-12480, 2021.

[36] X. Jiang, X. Liu, M. Wu, Y. Ma, X. Xu, L. Chen, and N. Niu, "Facile off-on fluorescence biosensing of human papillomavirus using DNA probe coupled with sunflower seed shells carbon dots," *Microchemical Journal,* vol. 181, p. 107742, 2022.

[37] P. Supchocksoonthorn, N. Thongsai, H. Moonmuang, S. Kladsomboon, P. Jaiyong, and P. Paoprasert, "Label-free carbon dots from black sesame seeds for real-time detection of ammonia vapor via optical electronic nose and density functional theory calculation," *Colloids and Surfaces A: Physicochemical and Engineering Aspects,* vol. 575, pp. 118-128, 2019.

[38] K. Wang, C. Geng, F. Wang, Y. Zhao, and Z. Ru, "Urea-doped carbon dots as fluorescent switches for the selective detection of iodide ions and their mechanistic study," *RSC Advances,* 10.1039/D1RA04558J vol. 11, no. 44, pp. 27645-27652, 2021.

[39] R. Hu, L. Li, and W. J. Jin, "Controlling speciation of nitrogen in nitrogen-doped carbon dots by ferric ion catalysis for enhancing fluorescence," *Carbon,* vol. 111, pp. 133-141, 2017.

[40] A. B. Bourlinos, R. Zbořil, J. Petr, A. Bakandritsos, M. Krysmann, and E. P. Giannelis, "Luminescent surface quaternized carbon dots," *Chemistry of Materials,* vol. 24, no. 1, pp. 6-8, 2012.

[41] M. Zulfajri, S. Dayalan, W. Y. Li, C. J. Chang, Y. P. Chang, and G. G. Huang, "Nitrogen-doped carbon dots from averrhoa carambola fruit extract as a fluorescent probe for methyl orange," (in eng), *Sensors (Basel, Switzerland),* vol. 19, no. 22, 2019.

[42] J. Joseph, and A. A. Anappara, "White-light-emitting carbon dots prepared by the electrochemical exfoliation of graphite," *ChemPhysChem, v*ol. 18, no. 3, pp. 292-298, 2017.

[43] M. C. Ortega-Liebana, N. X. Chung, R. Limpens, L. Gomez, J. L. Hueso, J. Santamaria, and T. Gregorkiewicz, "Uniform luminescent carbon nanodots prepared by rapid pyrolysis of organic precursors confined within nanoporous templating structures," *Carbon,* vol. 117, pp. 437-446, 2017.

[44] S. D. Torres Landa, I. Kaur, and V. Agarwal, "Pithecellobium dulce leaf-derived carbon dots for 4-Nitrophenol and Cr(VI) detection," *Chemosensors*, vol. 10, no. 12,

[45] A. Q. Hassan, R. K. Barzani, K. M. Omer, B. R. Al-Hashimi, S. Mohammadi, and A. Salimi, "Dual-emitter polymer carbon dots with spectral selection towards nanomolar detection of iron and aluminum ions," *Arabian Journal of Chemistry,* vol. 14, no. 12, p. 103452, 2021.

[46] X. Huo, H. Shen, R. Liu, and J. Shao, "Solvent effects on fluorescence properties of carbon dots: implications for multicolor imaging," *ACS Omega,* vol. 6, no. 40, pp. 26499-26508, 2021.

[47] J. Lavanya, N. Gomathi, and S. Neogi, "Electrochemical performance of nitrogen and oxygen radio-frequency plasma induced functional groups on tri-layered reduced graphene oxide," *Materials Research Express,* vol. 1, no. 2, p. 025604, 2014.

[48] Y. Deng, J. Qian, Y. Zhou, and Y. Niu, "Preparation of N/S doped carbon dots and their application in nitrite detection," *RSC Advances,* 10.1039/D0RA10766B vol. 11, no. 18, pp. 10922-10928, 2021.

[49] Z. Huang, F. Lin, M. Hu, C. Li, T. Xu, C. Chen, and X. Guo, "Carbon dots with tunable emission, controllable size and their application for sensing hypochlorous acid," *Journal of Luminescence,* vol. 151, pp. 100-105, 2014.

[50] R. Wang, X. Wang, and Y. Sun, "One-step synthesis of self-doped carbon dots with highly photoluminescence as multifunctional biosensors for detection of iron ions and pH," *Sensors and Actuators B: Chemical,* vol. 241, pp. 73-79, 2017.

[51] S. Wei, X. Yin, H. Li, X. Du, L. Zhang, Q. Yang, and Dr. R. Yang, "Multi-color fluorescent carbon dots: Graphitized sp2 conjugated domains and surface state energy level Co-modulate band gap rather than size effects," *Chemistry – A European Journal,* vol. 26, no. 36, pp. 8129-8136, 2020.

[52] A. D. Wilson, and M. Baietto, "Applications and advances in electronic-nose technologies," (in eng), *Sensors (Basel, Switzerland),* vol. 9, no. 7, pp. 5099-5148, 2009.

[53] K. Druckenmüller, K. Günther, and G. Elbers, "Near-infrared spectroscopy (NIRS) as a tool to monitor exhaust air from poultry operations," *Science of The Total Environment,* vol. 630, pp. 536-543, 2018.

[54] R. Iwamoto, "Infrared and near-infrared study of the interaction of amide C═O with water in ideally inert medium," *The Journal of Physical Chemistry A,* vol. 114, no. 27, pp. 7398-7407, 2010.

[55] D.-C. Gu, M.-J. Zou, X.-X. Guo, P. Yu, Z.-W. Lin, T. Hu, Y-F. Wu, Y. Liu, J-H Gan, S-Q. Sun, X-C. Wang, and C-H. Xu, "A rapid analytical and quantitative evaluation of formaldehyde in squid based on Tri-step IR and partial least squares (PLS)," *Food Chemistry,* vol. 229, pp. 458-463, 2017.

[56] K. Rovina, J. M. Vonnie, S. N. Shaeera, S. X. Yi, and N. F. A. Halid, "Development of biodegradable hybrid polymer film for detection of formaldehyde in seafood products," *Sensing and Bio-Sensing Research,* vol. 27, p. 100310, 2020.

[57] S. W. C. Chung, and B. T. P. Chan, "Trimethylamine oxide, dimethylamine, trimethylamine and formaldehyde levels in main traded fish species in Hong Kong," *Food Additives & Contaminants: Part B,* vol. 2, no. 1, pp. 44-51, 2009.

[58] Q. Liu, S. Fan, L. Fu, C. Liu, J. Xu, and W. Tang, "Carbon quantum dot modified electrospun TiO_2 nanofibers for flexible formaldehyde gas sensor under UV illumination at room temperature," *Diamond and Related Materials,* vol. 140, p. 110542, 2023.

[59] Y. Tachapermpon, P. Muangphrom, P. Pataranutaporn, W. Chaiworn, and W. Surareungchai, "Fluorescent carbon dots based phytosensor for indoor formaldehyde pollution monitoring," *Plant Nano Biology,* vol. 2, p. 100015, 2022.

[60] Y. Li, M. Hu, K. Liu, S. Gao, H. Lian, and C. Xu, "Lignin derived multicolor carbon dots for visual detection of formaldehyde," *Industrial Crops and Products,* vol. 192, p. 116006, 2023.

[61] M. M. Ayad, M. E. Abdelghafar, N. L. Torad, Y. Yamauchi, and W. A. Amer, "Green synthesis of carbon quantum dots toward highly sensitive detection of formaldehyde vapors using QCM sensor," *Chemosphere,* vol. 312, p. 137031, 2023.

[62] S. Zhang, X. Fan, S. Jiang, D. Yang, M. Wang, T. Liu, X. Shao, S. Wang, G. Hu, and Q. Yue, "High sensitive assay of formaldehyde using resonance light scattering technique based on carbon dots aggregation," *Arabian Journal of Chemistry,* vol. 16, no. 6, p. 104786, 2023.

[63] W. A. Amer, A. F. Rehab, M. E. Abdelghafar, N. L. Torad, A. S. Atlam, and M. M. Ayad, "Green synthesis of carbon quantum dots from purslane leaves for the detection of formaldehyde using quartz crystal microbalance," *Carbon,* vol. 179, pp. 159-171, 2021.

[64] J. Qu, X. Zhang, Y. Liu, Y. Xie, J. Cai, G. Zha, and S. Jing, "N, P-co-doped carbon dots as a dual-mode colorimetric/ ratiometric fluorescent sensor for formaldehyde and cell imaging via an aminal reaction-induced aggregation process," *Microchimica Acta,* vol. 187, no. 6, p. 355, 2020.